

Quantum hard rods: Critical behavior and conformal invariance

Ferenc Iglói*

Instituut voor Theoretische Fysica, Katholieke Universiteit Leuven, B-3030 Leuven, Belgium

(Received 1 February 1989)

The critical properties of one-dimensional quantum Ising models with near-neighbor exclusion (hard rods) are studied by finite-size scaling and conformal invariance. For dimers (rods with length $m=2$) the system exhibits an Ising-type critical point, while for $m \geq 3$ the system undergoes a first-order phase transition. The operator content of the critical Hamiltonian of hard dimers has been determined for different boundary conditions and identification with the sectors of the Ising model has been done. Using our results, we propose a phase diagram for the quantum Ising model with multispin interaction in the presence of transverse and longitudinal fields.

I. INTRODUCTION

Models with nearest-neighbor exclusion have been introduced to describe the fluid-solid phase transition of systems of rigid molecules¹ and to model the order-disorder transition of adsorbed monolayers on two-dimensional surfaces.² For such models in two-dimensions, the first exact results have been achieved for close-packing problems (dimers, dumbbells).³⁻⁵ The most famous exact result in this field is due to Baxter,⁶ who solved the hard hexagon model (the triangular lattice gas with nearest-neighbor exclusion), showing that the system undergoes a second-order phase transition characterized by the critical exponents conjectured for the three-state Potts model.⁷ It is interesting, that the hard-square model (square-lattice gas with nearest-neighbor exclusion) has no exact solution yet, although analytical, numerical, and series studies⁸⁻¹¹ accurately show that the system obeys an Ising-type critical point. The hard-square model is equivalent to the high-field limit of the antiferromagnetic (AF) square-lattice Ising model in a field, and the numerical results have been used to check the accuracy of the Müller-Hartmann-Zittartz formula.¹² The generalized hard-square model with second-neighbor attraction shows interesting features: a line of tricritical points and a surface of first-order transition.¹³⁻¹⁵

In this paper we introduce a one-dimensional quantum analogy of these models, which we refer to as quantum hard rods. (The classical one-dimensional hard-rod system is the subject of intensive investigations due to its interesting dynamical behavior.¹⁶)

The Hamiltonian of the system is defined as

$$H = - \sum_i \sigma_i^z - h \sum_i \sigma_i^x + J_1 \sum_i (\sigma_i^z + 1)(\sigma_{i+1}^z + 1) + J_2 \sum_i (\sigma_i^z + 1)(\sigma_{i+2}^z + 1) + \dots, \quad (1.1)$$

where σ_i^z, σ_i^x are Pauli matrices at site i , and $J_i = \infty$ for $i=1, 2, \dots, m-1$, and it is zero for $i \geq m$. According to H (1.1), two up spins are separated by at least a distance of m ; thus, to each up spin a hard rod with length m can

be assigned, and the Hamiltonian (1.1) describes the absorption of these particles on the chain. Another possible interpretation of (1.1) is the description of the association-dissociation process of linear molecules with m atoms on a chain in the presence of an electric field.

The Hamiltonian (1.1) is equivalent to the $h_l \rightarrow 0$ limit of the following multispin-coupling model:

$$H_M = (-1)^m \sum_i \prod_{j=1}^m \sigma_{i+j-1}^z - h_l \sum_i \sigma_i^z - h_t \sum_i \sigma_i^x. \quad (1.2)$$

First we note, that this model for $h_l=0$ exhibits a phase transition at $h_t=1$ (Refs. 17 and 18), where the degeneracy of the ground state is lifted by a factor of 2^{m-1} , and the transition is continuous for $m=2$ [Ising-type (Ref. 19)] and for $m=3$ [four-state Potts type (Refs. 20-23)], while it is of first order for $m \geq 4$ (Refs. 24 and 25). In the presence of a negative longitudinal field the schematic phase diagram is sketched in Fig. 1. Along the phase transition line which terminates at $h_t=0$, $h_l=-m$, the ground-state degeneracy changes by a factor of m ; thus for $m \geq 3$ one expects a different type of critical behavior than is present for $h_l=0$. At $h_t=0$, H_M describes a classical system, the ground state of which is infinitely degenerate at $h_l=-m$: all of those states have the same energy in which the distance between neighboring up spins is at least m . This degeneracy is solved up by switching on the h_t field, and the secular equations of the first-order degenerate perturbation calculation are equivalent to the quantum-hard-rod problem in (1.1), where $h = h_t / (h_l + m)$ measures the slope of the transition line in the limit $h_l \rightarrow 0, h_l \rightarrow -m$.

The H_M Hamiltonian for $m=3$ has been numerically studied by Penson *et al.*²⁶ Three-state Potts critical behavior is found in accordance with the ground-state degeneracy of the ordered phase, but the fluctuations in the numerical data was so strong for $-3 < h_l < -2$ that no conclusion could be drawn in that region.

Our aim in the present paper is to study the phase transition of the hard-rod model (1.1) and at the same time to complete the phase diagram of the multispin-coupling Hamiltonian (1.2). The structure of the paper is the following. In Sec. II the phase transition point and the criti-

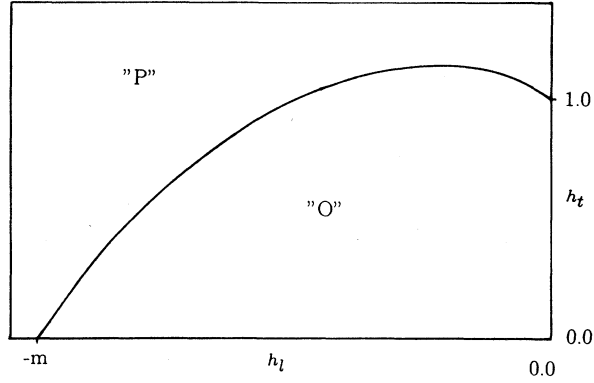


FIG. 1. Schematic phase diagram of the Ising model with multispin coupling in the presence of transverse and longitudinal fields Eq. (1.2). The degeneracy of the ground state is lifted by a factor of m along the phase transition line separating the paramagnetic (“P”) and the ordered (“O”) regions. The quantum hard-rod problem Eq. (1.1) is obtained in the limit $h_t \rightarrow 0$, and the slope of the phase transition curve at $h_l = -m$ corresponds to the critical point h_c of H .

cal behavior of (1.1) is determined by finite-size scaling (FSS) (Ref. 27). In Sec. III the FSS spectrum of the $m=2$ critical Hamiltonian is investigated, and the operator content of the model is determined for different boundary conditions (BC’s) by applying conformal invariance. Finally, Sec. IV contains a discussion.

II. PHASE TRANSITION IN THE SYSTEM

The translation invariance of the ground state of H (1.1) is spontaneously broken at a critical value of $h = h_c$, and for $h < h_c$ the ground state is m -fold degenerate, antiferromagneticlike ordered. To locate the phase transition point and to determine the critical behavior of the models we use finite-size scaling.²⁷ In this method the first step is the calculation of the energy of the ground state $E_0(L)$ and of the first excited state $E_1(L)$ for finite chains with L lattice sites by the Lanczos tridiagonalization scheme. The dimension of the eigenvalue matrix (D_L^m) follows a simple rule. Since the possible states are of two kinds depending on whether the first spin is $|\downarrow\rangle$ or it is $|\uparrow\rangle$ (i.e., a rod starts with length m) we can write

$$D_L^m = D_{L-1}^m + D_{L-m}^m. \quad (2.1)$$

Thus, D_L^m asymptotically behaves as $D_L^m = x_m^L$ with x_m the solution of $x_m^m = x_m^{m-1} + 1$; $x_2 = (1 + \sqrt{5})/2 = 1.618 \dots$ the golden ratio, $x_3 = 1.4656$. Since D_L^m increases very slowly with the size of the lattice as the dimension of the eigenvalue problem of H_M in (1.2), which is 2^L independently of m , we can investigate much larger systems. The maximal lattices in our calculation were $L=22$ and $L=30$ for $m=2$ and $m=3$, respectively. [We previously mentioned that Penson *et al.*²⁶ have diagonalized H_M (1.2) for $m=3$ up to $L=15$.] The next step in the FSS analysis is to locate the critical point h_c as the limit for $L, L' \rightarrow \infty$, the series of FSS fixed points h_L^* solution of

$$F_L(h_L^*) = F_{L'}(h_L^*), \quad (2.2)$$

where

$$F_L(h) = L[E_1(L) - E_0(L)]$$

is the scaled gap. To determine the limit of the finite-size data different sequence extrapolation methods have been developed.^{28–30}

We mention that this method can be successfully applied to locate a first-order phase transition point, too. In this case the presence of a so-called hybridization gap^{31,32} in finite systems at the phase transition point signals the crossing of energy levels in infinite systems. Since the hybridization gap vanishes exponentially with increasing system size, the scaled gap goes to zero at the phase transition point; however, the h_L^* series separates the ordered [$F_L(h) \rightarrow \infty$] and the disordered [$F_L(h) \rightarrow 0$] regions in this case, too.

Next, we turn to specifying the values of the system size. Due to the AF-like order the symmetry of the states for finite chains depends on

$$l = L \pmod{m} = 1, 2, \dots, m-1,$$

and the degeneracy of the ground state for infinite systems is preserved only if $L = km$, with $k = 1, 2, \dots$. Therefore in the FSS analysis we use $L = km$, $L' = L + m$. We note that for different values of l different boundary conditions are defined with different operator content of the Hamiltonian. Having located the critical point the correlation length or gap exponent $\nu = 1/y_t$ may be determined from the scaling law:²⁷

$$\left. \frac{dF_L}{dh} \right|_{h=h_c} \propto L^{y_t}. \quad (2.3)$$

In practice a finite-size estimate for y_t can be obtained from the series

$$y_{t,L} = \left[\ln \left(\frac{dF_{L'}}{dh} / \frac{dF_L}{dh} \right) \right]_{h=h_L^*} / \ln(L'/L). \quad (2.4)$$

A first-order transition is controlled by a discontinuity fixed point³³ with $y_t = 2$ in two dimensions. In the following we present the numerical results for $m=2$ and 3.

A. Results for $m=2$

The numerical calculations have been performed for finite chains with even lattice sites up to $L=22$. The FSS fixed points, the value of the scaled gap at these points, and the difference in the derivative of the scaled gaps

$$\Delta \dot{F}_L = \left. \frac{dF_L'}{dh} \right|_{h=h_L^*} - \left. \frac{dF_L}{dh} \right|_{h=h_L^*} \quad (2.5)$$

are presented in Table I. One can see that the different series quickly converge to their limit. As an example we present the result of the van den Broeck–Schwartz (VBS) extrapolation algorithm²⁸ for the FSS fixed points in Table II, which leads to an estimate

$$h_c = 1.526492 \pm 0.000005.$$

TABLE I. The FSS fixed points, the value of the scaled gap at these points, and the difference in the derivative of the scaled gaps Eq. (2.5) for the hard dimer model.

L	h_L^*	$F_L(h_L^*)$	$\Delta\dot{F}_L$
2	2.090 449	2.120 890	0.482 437
4	1.588 491	1.247 216	0.487 720
6	1.545 843	1.157 752	0.474 913
8	1.534 968	1.130 190	0.468 819
10	1.530 944	1.118 182	0.465 578
12	1.529 116	1.111 896	0.463 669
14	1.528 167	1.108 201	0.462 456
16	1.527 626	1.105 847	0.461 639
18	1.527 295	1.104 256	0.461 063
20	1.527 081	1.103 131	0.460 643

The extrapolation of the other two quantities in Table II gives

$$F(h_c) = 1.098\ 51, \quad \Delta\dot{F} = 0.4586. \quad (2.6)$$

Since $\Delta\dot{F}$ approaches a finite value according to (2.3) the correlation length exponent $\nu = 1$ and the transition is an Ising type, as expected from the ground-state degeneracy. To obtain a more transparent picture we define the density of hard rods as

$$\rho = 1 + \langle \sigma^z \rangle \quad (2.7)$$

and plot this quantity as a function of h in Fig. 2. As shown, ρ decreases monotonically with increasing h from $\rho = 1$, but due to quantum fluctuations its value remains finite even at the maximally disordered point: For $h \rightarrow \infty$, $\rho = 0.391\ 67$. At the critical point $\rho_c = 0.689\ 17$, and according to numerical studies, the first derivative of ρ has a logarithmic singularity around the critical point, as to $\langle \sigma^z \rangle$ for the Ising model.¹⁹ We note that in the hard dimer model the first neighbor correlations are related to the one-site expectational values since

$$1 + \sigma_i^z + \sigma_{i+1}^z + \sigma_i^z \sigma_{i+1}^z = 0. \quad (2.8)$$

B. Results for $m=3$

In this case the numerical calculations have been performed for finite chains up to $L=30$. The FSS fixed points, the value of the scaled gap in these points, as well as the estimates for the y_t critical exponent (2.4) are

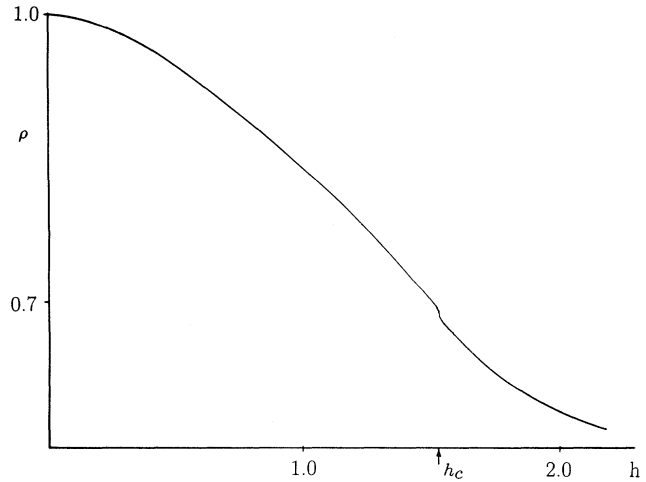


FIG. 2. The density of hard dimers Eq. (2.7) extrapolated from finite lattice data. The first derivative of ρ has a logarithmic singularity at the critical point.

presented in Table III. Our first observation when comparing the results of the $m=3$ model to the results of the $m=2$ model is the much slower convergence of the data. The series of FSS fixed points seems to approach their limit $h_c = 1.013 \pm 0.001$ like $1/L$, in contrast to the usual correction terms for periodic BC $O(1/L^3) - O(1/L^2)$ (Ref. 27). It is extremely difficult to obtain a convincing extrapolation value for the y_t exponent. Concerning the ground-state degeneracy of the ordered phase of the model, three different types of critical behavior are possible: (i) critical three-state Potts model ($y_t = 1.2$) (Ref. 7), (ii) tricritical three-state Potts model ($y_t = \frac{12}{7} = 1.714$) (Ref. 7), and (iii) first-order transition with discontinuity fixed point ($y_t = 2$). The numerical values in Table III rule out the possibility that the model belongs to the universality class of the critical three-state Potts model, but it is impossible to decide between the two other cases purely on the basis of the $y_{t,L}$ series. Therefore, we perform other independent estimates to determine the order of the transition.

First let us study the limit value of the scaled gap. The F_L values in Table III seems to tend to zero. Supposing an exponential decay of the form $F_L^* \propto \exp(-\alpha L)$ the estimate $\alpha = 0.007 - 0.005$ can be obtained. A similar exponent can be deduced from the series of the scaled gaps

TABLE II. VBS extrapolants for the critical point for the hard dimer model.

2.090 448 8					
1.588 490 7	1.541 883 0				
1.545 842 9	1.531 245 5	1.526 546 0			
1.534 967 8	1.528 581 0	1.526 499 3	1.526 492 2		
1.530 944 1	1.527 593 1	1.526 493 2	1.526 492 2	1.526 492 2	
1.529 115 8	1.527 142 6	1.526 492 3	1.526 492 6	1.526 492 5	
1.528 166 8	1.526 908 1	1.526 492 7	1.526 492 4		
1.527 625 7	1.526 774 2	1.526 490 2			
1.527 294 9	1.526 692 0				
1.527 081 3					

TABLE III. The FSS fixed points, the value of the scaled gap at these points, and the finite lattice estimate for the ν , exponent Eq. (2.4) for the $m=3$ model.

L	h_L^*	$F_L(h_L^*)$	$\nu_{L,L}$
3	1.568 936	1.895 631	0.579 611
6	1.153 499	0.957 429	0.897 600
9	1.099 301	0.804 800	1.019 746
12	1.077 388	0.727 393	1.093 275
15	1.065 027	0.674 379	1.143 939
18	1.056 904	0.633 258	1.181 695
21	1.051 088	0.599 269	1.211 424
24	1.046 688	0.570 109	1.235 823
27	1.043 229	0.544 478	1.256 509

at $h = h_c$. These results show the presence of a hybridization gap,^{31,32} thus they are in favor of a weakly first-order phase transition in the system.

In order to obtain an independent evidence on the order of the transition, we determined the latent heat. In Table IV the first derivatives of the ground-state energy are tabulated, in the first column at $h = h_c$ and in the next two at the FSS fixed points. (The second and third columns contain results for chains with spins L and $L + 3$, respectively.) The second and third series have the same limit,

$$D_2 = \lim_{L \rightarrow \infty} \frac{1}{L} \frac{\delta E_0(L)}{\delta h} \Big|_{h=h_L^*} = \frac{\delta \epsilon_0}{\delta h} \Big|_{h=h_c+}, \quad (2.9)$$

while the limit of the first series is

$$D_1 = \lim_{L \rightarrow \infty} \frac{1}{L} \frac{\delta E_0(L)}{\delta h} \Big|_{h=h_c} = \frac{1}{2} \left[\frac{\delta \epsilon_0}{\delta h} \Big|_{h=h_c+} + \frac{\delta \epsilon_0}{\delta h} \Big|_{h=h_c-} \right]. \quad (2.10)$$

The latent heat determined from these limits as

$$\Delta L = \frac{\delta \epsilon_0}{\delta h} \Big|_{h=h_c-} - \frac{\delta \epsilon_0}{\delta h} \Big|_{h=h_c+} = 2(D_1 - D_2) \quad (2.11)$$

is zero for second-order transitions, while it is finite for

first-order ones. In our case from the values of Table IV one can calculate a very small latent heat $\Delta L = 0.004$ (which is on the order of the latent heat of the $Q=5-6$ state Potts model³⁴), but its value is comparable with the error of the estimate. Thus, we can conclude that the transition of the $m=3$ model is very probably of weakly first order; however, the estimated latent heat of the transition is very small; thus the possibility of a second-order transition with very strong confluent singularity cannot be excluded. (We note that the classical hard-square model with diagonal attraction also exhibits a first-order transition.¹⁴)

III. OPERATOR CONTENT OF THE $m=2$ MODEL

Conformal invariance supplies a very efficient method to determine the anomalous dimensions of critical operators by calculating the FSS spectrum of the critical Hamiltonian for different boundary conditions.³⁵ For toroidal BC (periodic, antiperiodic, twisted) the dispersion relation for an excited state obeys the form

$$E - E_0 = \frac{2\pi}{L} \xi [\Delta + r + (\bar{\Delta} + \bar{r})], \quad (3.1)$$

$$P - P_0 = \frac{2\pi}{L} [\Delta + r - (\bar{\Delta} + \bar{r})], \quad (3.2)$$

where $(\Delta, \bar{\Delta})$ characterize a primary scaling operator, where $x = \Delta + \bar{\Delta}$ is the scaling dimension and $s = \Delta - \bar{\Delta}$ is the spin, r, \bar{r} are non-negative integers, ξ is a normalizing constant (the so-called sound velocity³⁶), and E_0 denotes the ground-state energy of the Hamiltonian with periodic BC. The finite-size correction to E_0 is universal.^{37,38}

$$E_0(L) = L \xi \left[\epsilon_0 - \frac{\pi c}{6L^2} + \dots \right], \quad (3.3)$$

where c is the central charge of the Virasoro algebra. For a free boundary condition, Eqs. (3.1) and (3.3) are modified as

$$E - E_0 = \frac{\pi}{L} \xi (\Delta + r), \quad (3.4)$$

$$E_0(L) = L \xi \left[\epsilon_0 + \frac{\epsilon_1}{L} - \frac{\pi c}{24L^2} + \dots \right]. \quad (3.5)$$

TABLE IV. The first derivative of the ground-state energy density at the bulk phase transition point (first column) and in the FSS fixed points (second and third columns). The extrapolated values are in the last row.

L	$-\dot{\epsilon}_0(L, h_c)$	$-\dot{\epsilon}_0(L, h_L^*)$	$-\dot{\epsilon}_0(L + 3, h_L^*)$
3	0.501 577	0.417 320	0.541 829
6	0.343 291	0.355 359	0.370 223
9	0.319 585	0.338 368	0.342 620
12	0.310 628	0.330 066	0.331 659
15	0.305 927	0.324 906	0.325 566
18	0.302 998	0.321 270	0.321 537
21	0.300 975	0.318 507	0.318 591
24	0.299 479	0.316 302	0.316 296
27	0.298 319	0.314 483	0.314 429
30	0.297 387		
extrapolation	0.2878±0.0002	0.290±0.002	0.290±0.002

Our Hamiltonian (1.1) is different from that of the usual models with nearest-neighbor ferromagnetic interaction, while it has a nontranslationally invariant ground state and cannot be defined as an antiperiodic-type BC. Furthermore, as already mentioned, the parity of the length of the chain defines different boundary conditions. Thus, in order to define the reference energy values E_0 in (3.3) and (3.5), we first determine the finite-size behavior of the ground-state energy for different BC's.

(a) Periodic BC even lattice

$$E_0^{P,E}(L) = L\xi \left[\epsilon_0 - \frac{c\pi}{6L^2} + \dots \right], \quad (3.6)$$

where $c=0.50000$, $\epsilon_0=-0.15694$, and the sound velocity determined from the distance of the equidistant levels is $\xi=2.7973$. The accuracy of these figures is about five digits.

(b) Periodic BC odd lattice:

$$E_0^{P,O}(L) = L\xi \left[\epsilon_0 + \frac{\pi}{6L^2} + \dots \right]. \quad (3.7)$$

(c) Free BC even lattice:

$$E_0^{F,E}(L) = L\xi \left[\epsilon_0 + \frac{\epsilon_1}{L} + \frac{23}{2} \frac{\pi}{24L^2} + \dots \right], \quad (3.8)$$

where the surface energy is given by $\epsilon_1=-0.47809$.

(d) Free BC odd lattice:

$$E_0^{F,O}(L) = L\xi \left[\epsilon_0 + \frac{\epsilon_1}{L} - \frac{c\pi}{24L^2} + \dots \right]. \quad (3.9)$$

Comparing (3.6) and (3.7) we can conclude that the ground state of even rings is always lower than that of odd rings, but the situation is just the opposite for free chains, Eqs. (3.8) and (3.9). The asymptotic behavior of $E_0^{P,E}(L)$ and $E_0^{F,O}(L)$ corresponds to (3.3) and (3.5), respectively, with conformal anomaly $c=\frac{1}{2}$ characteristic for the Ising model.³⁵ Furthermore, the finite-size correction for odd rings in (3.7) is the same as that of the Ising model with antiperiodic BC (Ref. 39). In the following we use $E_0^{P,E}(L)$ and $E_0^{F,O}(L)$ as reference energy for periodic BC in (3.3) and for free BC in (3.5), respectively. (We note that similar strategy has been used by Alcaraz *et al.*⁴⁰ for the XXZ model.)

Next we present the operator content of the model based on a comparison of the numerically determined levels of the spectra with the known operator content of the different sectors of the Ising model.^{35,41} For periodic BC due to the AF order, the low-lying excitations are of two kinds: with momentum $O(1/L)$ and with $\pi+O(1/L)$. Thus we have four sectors depending on the parity of the length of the chain (E, P) and on the value of the momentum ($0, \pi$). The first few levels of the spectrum of the different sectors are presented in Fig. 3. These can be identified to the levels of the spectra of the Ising model with toroidal BC (Refs. 35 and 41) using the following correspondence:

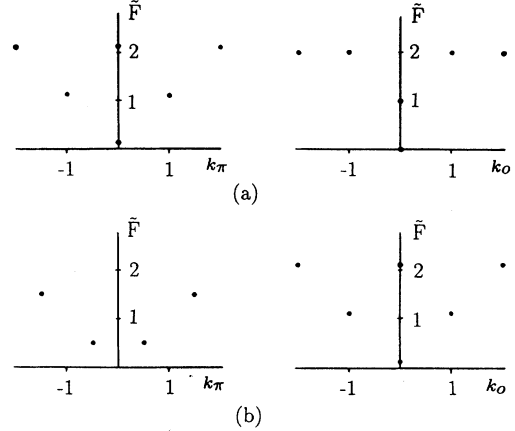


FIG. 3. The spectrum of the critical hard dimer system in the FSS limit for periodic boundary conditions: (a) even chains and (b) odd chains. The notations are $\tilde{F} = (E - E_0)\xi L / 2\pi$, E_0 is the ground-state energy for even rings, $k_0 = P(L/2\pi)$ and $k_\pi = (P - \pi)(L/2\pi)$ measure the momenta in the two different sectors (see the text).

Hard dimer	Ising model
Even chain	Periodic BC
Odd chain	Antiperiodic BC
$P = O(1/L)$	Magnetic excitations
$P = \pi + O(1/L)$	Energy excitations

Thus, the operator content of the different sectors are the following. (a) Periodic BC even lattice: The $P = O(1/L)$ sector is given by the irreducible representation $(0,0)$ and $(\frac{1}{2}, \frac{1}{2})$, while the $P = \pi + O(1/L)$ sector is given by $(\frac{1}{16}, \frac{1}{16})$. (b) Periodic BC odd lattice: The $P = O(1/L)$ sector is given by the irreducible representations $(0, \frac{1}{2})$ and $(\frac{1}{2}, 0)$, while the $P = \pi + O(1/L)$ sector is given by $(0,0)$ and $(\frac{1}{2}, \frac{1}{2})$. For free BC one Virasoro algebra describes the spectrum, which is the following. (c) Free BC even lattice:

$$E - E_0 = \frac{\pi}{L} \xi \left(\frac{1}{2} + r \right). \quad (3.10)$$

The spectrum is given by the irreducible representation $\Delta = \frac{1}{2}$. (d) Free BC odd lattice:

$$E - E_0 = \frac{\pi}{L} \xi (2 + r). \quad (3.11)$$

The spectrum is given by the irreducible representation $\Delta = 2$. Thus, the even and odd sectors correspond to the magnetization and the energy sectors of the Ising model,⁴² respectively.

IV. DISCUSSION

In this paper the phase transition of the quantum hard-rod system (1.1) has been studied, where the cooperative behavior of the system is forced by an exclusion principle rather than by nearest-neighbor attraction. The model exhibits a fluid-solid type phase transition, where the ordered phase has an antiferromagnetic-

like long-range order. The phase transition for $m=2$ is found continuous with Ising critical exponents, while it is of weakly first order for $m=3$. Since the ground-state degeneracy of the ordered phase is m and by increasing ground-state degeneracy the latent heat of the transition generally increases,³⁴ we expect first-order transition for $m > 3$, too.

The hard-rod Hamiltonian is a special limit of the multispin coupling Ising model with transverse and longitudinal fields Eq. (1.2), thus we can use our results to comment on the phase diagram of this model (Fig. 1). For $m=2$ along the whole transition line, the phase transition is an Ising type, while for $m=3$ we expect a (three-state Potts) tricritical point separating the continuous (three-state critical Potts) and first-order transition regions. For $m=4$ two possibilities may occur: either first-order transition along the whole line, or four-state Potts transition for $h_l \geq h_l^*$ and first order for $h_l < h_l^*$ similarly to the case of the four-state Potts lattice gas.⁴³ For $m > 4$ the phase

transition along the whole line is of first order.

Turning back to the hard dimer problem, we have determined the operator content of the critical Hamiltonian for different boundary conditions and we have identified them with those of the Ising model. For the hard dimer model due to the quick convergency of the numerical data one might have hope of the existence of an exact solution. However, it is still not very likely, since in that case one should be able to solve the problem of the antiferromagnetic quantum Ising chain in a field (1.2); furthermore, its classical analogy, the hard-squares model, is still lacking an exact solution.

ACKNOWLEDGMENTS

This work has been supported by the Research Foundation (Onderzoeksfonds) of the University of Leuven. The author is indebted to R. Dekeyser for his hospitality in Leuven.

*On leave of absence from Institut für Theoretische Physik, Universität zu Köln, D-5000 Köln 41, Federal Republic of Germany.

†Permanent address: Central Research Institute for Physics, P.O. Box 49, H-1525 Budapest 114, Hungary.

¹L. K. Runnels, in *Phase Transitions and Critical Phenomena*, edited by C. Domb and M. S. Green (Academic, London, 1972), Vol. 2.

²M. Schick, *Prog. Surf. Sci.* **11**, 245 (1981).

³P. W. Kasteleyn, *Physica* **27**, 1209 (1961).

⁴M. E. Fisher, *Phys. Rev.* **124**, 1664 (1961).

⁵J. L. Hock and R. B. McQuistan, *J. Chem. Phys.* **83**, 3626 (1985).

⁶R. J. Baxter, *J. Phys. A* **13**, L61 (1980).

⁷M. P. M. den Nijs, *J. Phys. A* **12**, 1857 (1979).

⁸D. S. Gaunt and M. E. Fisher, *J. Chem. Phys.* **43**, 2840 (1965).

⁹L. K. Runnels and L. L. Combs, *J. Chem. Phys.* **45**, 2482 (1966).

¹⁰R. J. Baxter, I. G. Enting, and S. K. Tsang, *J. Stat. Phys.* **22**, 465 (1980).

¹¹P. A. Pearce and K. A. Seaton, *J. Stat. Phys.* **53**, 1061 (1988).

¹²E. Müller-Hartmann and J. Zittartz, *Z. Phys. B* **27**, 261 (1977).

¹³D. A. Huse, *Phys. Rev. Lett.* **49**, 1121 (1982).

¹⁴R. J. Baxter and P. A. Pearce, *J. Phys. A* **16**, 2239 (1983).

¹⁵N. C. Bartelt, T. L. Einstein, and L. D. Roelofs, *Phys. Rev. B* **34**, 1616 (1986).

¹⁶Ch. Foidl, P. Kasperkovitz, and O. J. Eder, *J. Phys. A* **20**, 2497 (1987).

¹⁷L. Turban, *J. Phys. C* **15**, L65 (1982).

¹⁸K. A. Penson, R. Jullien, and P. Pfeuty, *Phys. Rev. B* **26**, 6334 (1982).

¹⁹P. Pfeuty, *Ann. Phys. (N.Y.)* **57**, 79 (1970).

²⁰H. W. J. Blöte, *J. Phys. A* **20**, L35 (1987).

²¹F. C. Alcaraz and M. N. Barber, *J. Phys. A* **20**, 179 (1987).

²²C. Vanderzande and F. Iglói, *J. Phys. A* **20**, 4539 (1987).

²³F. Iglói, *J. Phys. A* **20**, 5319 (1987).

²⁴F. Iglói, D. Kapor, M. Škrinjar, and J. Sólyom, *J. Phys. A* **19**, 1189 (1986).

²⁵F. C. Alcaraz, *Phys. Rev. B* **34**, 4885 (1986).

²⁶K. A. Penson, J. M. Debierre, and L. Turban, *Phys. Rev. B* **37**, 7884 (1988).

²⁷M. N. Barber, in *Phase Transitions and Critical Phenomena*, edited by C. Domb and J. L. Lebowitz (Academic, London, 1983), Vol. 8.

²⁸J. M. van den Broeck and L. W. Schwartz, *SIAM (Soc. Ind. Appl. Math.) J. Math. Anal.* **10**, 658 (1979).

²⁹R. Bulirsch and J. Stoer, *Num. Math.* **6**, 413 (1964).

³⁰F. Beleznyay, *J. Phys. A* **19**, 551 (1986).

³¹F. Iglói and J. Sólyom, *J. Phys. C* **16**, 2833 (1983).

³²C. J. Hamer, *J. Phys. A* **16**, 3085 (1983).

³³B. Nienhuis and M. Nauenberg, *Phys. Rev. Lett.* **35**, 477 (1975).

³⁴R. J. Baxter, *J. Phys. C* **6**, L445 (1973).

³⁵J. Cardy, in *Phase Transitions and Critical Phenomena*, edited by C. Domb and J. L. Lebowitz (Academic, London, 1987), Vol. 11.

³⁶G. von Gehlen, V. Rittenberg, and H. Ruegg, *J. Phys. A* **19**, 107 (1986).

³⁷H. W. J. Blöte, J. Cardy, and M. P. Nightingale, *Phys. Rev. Lett.* **56**, 742 (1986).

³⁸I. Affleck, *Phys. Rev. Lett.* **56**, 746 (1986).

³⁹T. W. Burkhardt and I. Guim, *J. Phys. A* **18**, L33 (1985).

⁴⁰F. C. Alcaraz, M. Baake, U. Grimm, and V. Rittenberg, *J. Phys. A* **21**, L117 (1988).

⁴¹M. Henkel, *J. Phys. A* **20**, 995 (1987).

⁴²G. von Gehlen and V. Rittenberg, *J. Phys. A* **19**, L631 (1986).

⁴³B. Nienhuis, A. N. Berker, E. K. Riedel, and M. Schick, *Phys. Rev. Lett.* **43**, 737 (1979).